

1985 1986 1987 1988 1989 1990 1991 1992
1993 1994 1995 1996 1997 1998 1999 2000
2001 2002 2003 2004 2005 **2006** 2007 2008
2009 2010 2011 2012 2013 2014 2015 2016



Institute of Information Science, Academia Sinica

JISE

Journal of Information Science and Engineering

<http://www.iis.sinica.edu.tw/JISE/>

Special Issue for Selected Papers from CVGIP

Guest Editors: Cheng-Chin Chiang, Mark Liao,
Kuo-Chin Fan

Volume **22**
Number **3**
May **2006**

ISSN 1016-2364



Institute of Information and Computing Machinery, Taiwan

Contents

FOREWORD

SPECIAL ISSUE FOR SELECTED PAPERS FROM CVGIP

PAPERS

- 483 Copyright Protection against Print-and-Scan Operations by Watermarking for Color Images Using Coding and Synchronization of Peak Locations in Frequency Domain
Yen-Chung Chiu and Wen-Hsiang Tsai
- 497 Automatic White Balance for Digital Still Cameras
Varsha Chikane and Chiou-Shann Fuh
- 511 A Geometric Invariant Approach to Human Face Verification
Li-Wei He, Tsorng-Lin Chia and Chen-Kuei Yang
- 535 BCH Code-Based Robust Audio Watermarking in the Cepstrum Domain
Shi-Cheng Liu and Shinfeng D. Lin
- 545 Binarization Method Based on Pixel-level Dynamic Thresholds for Change Detection in Image Sequences
Hsu-Yung Cheng, Quen-Zong Wu, Kuo-Chin Fan and Bor-Shenn Jeng

REGULAR SECTION

PAPERS

- 559 A New Design for a Practical Secure Cookies System
Jong-Phil Yang and Kyung Hyune Rhee
- 573 A Classification Tree Based on Discriminant Functions
Been-Chian Chien, Jung-Yi Lin and Wei-Pang Yang
- 595 Building and Using Object-Oriented Frameworks for CAD Rapid Prototyping
Hewijin Christine Jiau and Kuo-Feng Ssu
- 611 Efficient One-time Signature Schemes for Stream Authentication
Yongsu Park and Yookun Cho
- 625 TeMeFr: Towards a Reuse-Based Development for Conference-Oriented Telemedicine Systems
Hewijin Christine Jiau, Jinghong Cox Chen, Kuo-Feng Ssu and Jim-Min Lin
- 641 Fast Octree Construction Endowed with an Error Bound Controlled Subdivision Scheme
Hong-Long Chou and Zen Chen
- 659 Profile-Based Lifetime Determination Schemes for Mobility Management in HMIPv6
Sun Ok Yang, SungSuk Kim and Chong-Sun Hwang
- 675 Storage Efficient Key Management Technique for Secure Multicasting
Ganapathi Padmavathi and Samukutty Annadurai

SHORT PAPERS

- 691 Authentication Protocols Using Hoover-Kausik's Software Token
Wei-Chi Ku and Hui-Lung Lee
- 701 Semi-fragile Image Authentication Using Real Symmetric Matrix
Ching-Tang Hsieh, Yeh-Kuang Wu, Chyi-Jang Lee and Hong-Yu Chen
-
- 713 Categories of Information Science and Engineering Areas
- 714 Call for Papers
- 715 Call for Papers for Software Publication Track
- 717 Manuscript Submission Form and Page Charge Agreement Form
- 719 Manuscript Submission Form (Software Publication Track)

Automatic White Balance for Digital Still Cameras*

VARSHA CHIKANE AND CHIOU-SHANN FUH

*Department of Computer Science and Information Engineering
National Taiwan University
Taipei, 106 Taiwan*

In recent years digital cameras have captured the camera market. Although the factors that consumer consider is the quality of the photographs produced. White balance is one of the methods used to improve the quality of the photographs. The basic white balance methods are, however powerless to handle all possible situations in the captured scene. In order to improve the white balance we divide this problem in three steps—white object purification, white point detection, and white point adjustment. The proposed method basically solves the problem of detecting the white point very well. The experimental results show that the proposed method can achieve superior result in both objective and subjective evaluative terms. The complexity of the proposed system is acceptable. The propose method can be easily applied to digital cameras to obtain good results.

Keywords: white balance, white point, gray world assumption, perfect reflector assumption, color balance

1. INTRODUCTION

Whenever a scene is captured by a digital camera, every pixel value of the recorded scene depends upon the 3-sensors response which is affected by the illuminant of that scene. A distinct color cast appears over the captured scene. This effect appears in the recorded image due to the color temperature of the light source. When a white object is illuminated with a low color temperature light source, the object in the captured image will be reddish in color. Similarly, if the white object is illuminated with a high color temperature light source, the object in the captured image will be bluish in color. To develop a white balance algorithm it is necessary to render the information about the illuminant of the scene.

Human vision may not be able to distinguish color differences caused by various light sources due to the “color constancy” of the human eye [1]. Colors remain constant through recognition even though they are viewed under different light sources. In summary, the mechanism employed in digital cameras to compensate for color differences caused by various light sources is white balance. This is the main focus of our investigation.

Received January 1, 2005; accepted June 30, 2005.

Communicated by C. C. Chiang, H. Y. Mark Liao and K. C. Fan.

* This research was supported in part by the National Science Council of Taiwan, R.O.C., under grants No. NSC 92-2213-E-002-072, by the EeRise Corporation, EeVision Corporation, Machvision, Tekom Technologies, Jeilin Technology, IAC, ATM Electronic, Primax Electronics, Arima Computer, and Lite-on.

2. BACKGROUND

The traditional methods used to adjust the white balance are described below.

2.1 Gray World Method (GWM)

The gray world assumption [2] states that, given an image with a sufficient amount of color variation, the average value of the RED, GREEN, and BLUE components of the image should average out to a common gray-value. With the gray world assumption, the average reflectance of the visible surfaces in every scene is assumed to be gray in order to estimate the spectral distribution of the illuminant. This method takes an image and scales its red, green, and blue color components to make the gray world assumption hold.

2.2 Perfect Reflector Method (PRM)

In the perfect reflector assumption [4], the *RGB* values of the “brightest” pixel in an image is the glossy or specular surface. For any white balancing algorithm, it is most important to gather information about the surfaces in the scene as well as the illuminant of the scene. The specularity is helpful for conveying a good amount of information about the illuminant as it reflects the actual color of the light source. It locates the reference white point by finding the pixel with the greatest luminance value and performs white balance adjustment according to the reference white point.

2.3 Fuzzy Rules Method (FRM)

In FRM [3], the image is converted from the *RGB* color space to the *YCrCb* color space, and the color’s characteristics in the *YCrCb* color space are used for white balance adjustment. The image is divided into 8 segments for more precise white balancing.

The fuzzy rules based on experimental results are described below:

1. The averages of C_r and C_b for each segment can be weighted with small values under the conditions of high-end and low-end luminance in order to keep the color components from becoming saturated and colorless.
2. The averages of C_r and C_b for each segment are weighted less for dark colors than bright colors.
3. When a large object or background occupies more than one segment, its color will dominate that segment. The ratios of C_r to C_b will be similar among adjacent segments. The given weighting for those segments that are uniform in chromatic color is kept small in order to avoid over-adjusting the color of the image.
4. If the ratio of C_r to C_b for a segment is roughly between -1.5 to -0.5 , then the probability of it being a white region increases, and the given weighting is the largest.

Besides these basic methods, another method is Chiou’s white balance [6] method, which tries to overcome the drawbacks of the basic methods.

2.4 Chiou's White Balance Method (CWBM)

This method is divided into three units: the white point detecting unit, white balance judging unit, and white balance adjusting unit.

2.4.1 White point detecting unit

In this unit the reference white points are detected. First the rough reference white pixels are detected from $YCrCb$ data of an image. Next, the pixels satisfying the Eq. (1) are picked up:

$$\sqrt{C_r^2 + C_b^2} \leq CH_{th}, \quad (1)$$

where threshold CH_{th} is equal to 60 and $\sqrt{C_r^2 + C_b^2}$ is the chromaticity value. Then, the pixels among the rough reference white pixels satisfying Eq. (2) are selected as precise reference white pixels:

$$\begin{aligned} R &\geq R_{th}, G \geq G_{th}, B \geq B_{th}, \\ |C_r| &\leq AB_r, |C_b| \leq AB_b, \\ R_l &\leq C_r/C_b \leq R_u, \end{aligned} \quad (2)$$

where, R_{th} , G_{th} , and B_{th} are thresholds picked up from the eightieth percentile of each component histogram. AB_r ($= 45$), and AB_b ($= 45$) are the absolute values of C_r , and C_b respectively and R_l ($= -1.25$), and R_u ($= -0.75$) are the lower and upper ranges of the ratio of C_r to C_b . Finally, the averages of the rough reference white pixels and precise reference white pixels are calculated as (R_r, G_r, B_r) and (R_p, G_p, B_p) , respectively.

2.4.2 White balance judging unit

This unit judges whether or not white balancing should be applied to the image. First, the R_{rough} , ratio of the rough reference white pixels to all of the pixels in the image, and $R_{precise}$, ratio of precise reference white pixels to all of the pixels in the image are calculated. Second, P_{rough} , defined as the prescribed proportion (0.2 in our experiment), and $P_{precise}$, defined as prescribed proportion (0.05 in our experiment). Finally, mode M_a is set to the value 0, 1, or 2 as shown in Fig. 1.

2.4.3 White balance adjusting unit

This unit adjusts the white balance according to the mode M_a . First, the scale factors are calculated according to the rough reference white point $(R_{rgain}, G_{rgain}, B_{rgain})$, and also according to the precise reference white point $(R_{pgain}, G_{pgain}, B_{pgain})$. If M_a is set to a value of 2, then the white balance is adjusted according to $(R_{pgain}, G_{pgain}, B_{pgain})$. If M_a is set to a value of 1, then select the minors between $(R_{rgain}, G_{rgain}, B_{rgain})$ and $(R_{pgain}, G_{pgain}, B_{pgain})$. Next if M_a is set to a value of 0 then white balance adjustment is not applied.

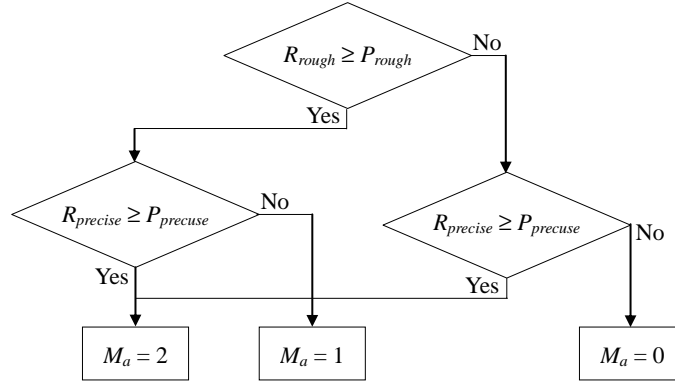


Fig. 1. Conditions for the setting mode.

For adjusting the extreme scale factors to obtain acceptable values, the sigmoid function shown in Eq. (3) is used:

$$Y = 1.05 * (1 + \tanh(X - 1.25)) + 0.4, \quad (3)$$

where X is the original scale factors and Y is the adjusted scale factors.

3. EXPERIMENTS

The Camera used in our experiments was set to the raw data mode to prevent image processing. The binary color interpolation scheme was applied to get *RGB* image data. To obtain more precise information about the color variation due to different light sources, we captured GretagMacbeth ColorChecker images under two conditions: varying the lighting conditions and varying the object conditions. To vary the lighting conditions, we captured GretagMacbeth ColorChecker images under standard light sources, as shown in Table 1, and also captured GretagMacbeth ColorChecker images under natural and household light sources.

Table 1. Light sources used in our experiments.

Light source	Daylight	Cool white	TL84	Inc. A'	Horizon
Color temperature (°K)	6500	4180	4100	2850	2300

To vary the object conditions, images were captured with and without ColorChecker. According to the CWBM and FRM, the white points were detected by using predefined values of C_r and C_b . In most cases, this predefined range for C_r and C_b was used to select another color pixel as the white point. Our main purpose was to use this small range to detect the white points in the desired image. Based on the experiments and our observations, we propose a new approach to white balance adjustment.

4. NEW APPROACH TO WHITE BALANCE ADJUSTMENT

We propose using a white object purification step. According to our observations in the experiments, if we purify the white object, then it is easy to detect in image. For this purpose, we apply histogram equalization to the desired image, extract information about the pixels belonging to the white point, and then use this information to select the white point in the original image. This new approach to white balancing involves the steps shown in Fig. 2.

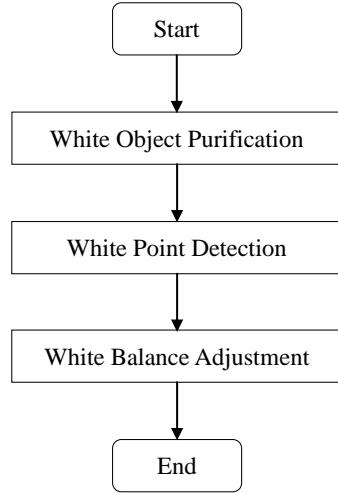


Fig. 2. The steps in the proposed method.

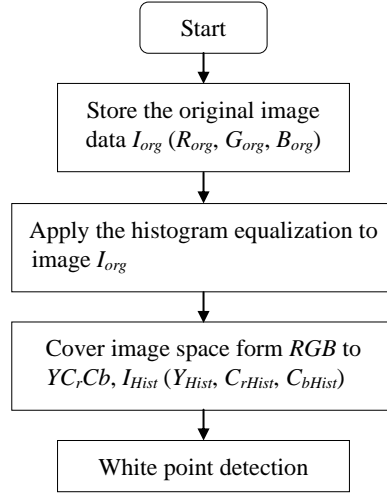


Fig. 3. Flowchart of white object purification.

4.1 White Object Purification

In the first step, white object purification is performed to purify the white object in such a way that the color cast over the white object is removed. Applying histogram equalization to the RGB channel separately results in removal of the color cast over the white object. After this step, white object detection can be performed more easily.

The flow chart of white object purification is shown in Fig. 3. First we store the original image data. Next we apply histogram equalization to each RGB channel separately. Then, $YCrCb$ color space data (Y_{Hist} , C_{rHist} , C_{bHist}) of histogram equalized image is calculated.

4.2 White Point Detection

In this step, first, we detect those pixels satisfying Eq. (4) as probable white pixels and the average of the selected probable white pixels is calculated as, Y_{Hist}^{avg} , C_{rHist}^{avg} , and C_{bHist}^{avg} . If no probable white pixel is detected, we stop for the white balancing process. The flow chart of the detection of probable white pixels is shown in Fig. 4.

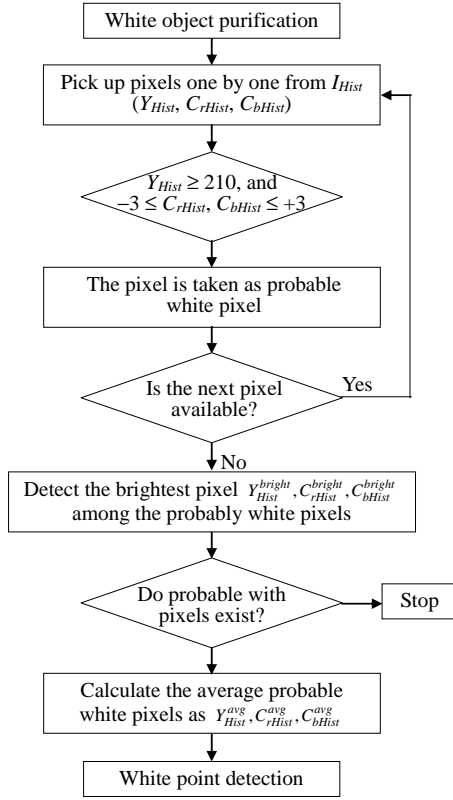


Fig. 4. Detection of probable white pixels.

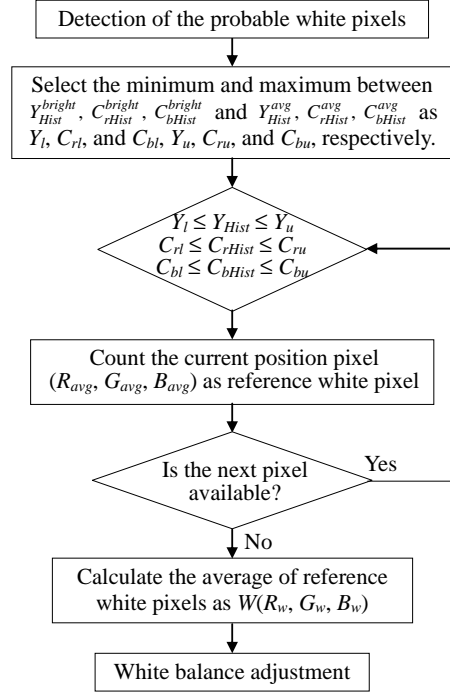


Fig. 5. White point detection.

$$Y_{Hist} \geq 210, \text{ and } -3 \leq C_{rHist}, C_{bHist} \leq +3. \quad (4)$$

Next, select the brightest pixels as Y_{Hist}^{bright} , C_{rHist}^{bright} , C_{bHist}^{bright} with highest Y_{Hist} value, and C_{rHist} , C_{bHist} values should be closest to zero, among all probable white pixels. Second, if the pixels, from the histogram-equalized image data satisfy Eq. (5), then select the corresponding position pixels from the original image in *RGB* color space data as reference white pixels.

$$Y_l \leq Y_{Hist} \leq Y_u, C_{rl} \leq C_{rHist} \leq C_{ru}, C_{bl} \leq C_{bHist} \leq C_{bu}, \quad (5)$$

where, Y_l , C_{rl} , and C_{bl} are lower limits: the minimum values between Y_{Hist}^{bright} , C_{rHist}^{bright} , C_{bHist}^{bright} and Y_{Hist}^{avg} , C_{rHist}^{avg} , C_{bHist}^{avg} . Similarly Y_u , C_{ru} , and C_{bu} are upper limits: the maximum values between Y_{Hist}^{bright} , C_{rHist}^{bright} , C_{bHist}^{bright} and Y_{Hist}^{avg} , C_{rHist}^{avg} , C_{bHist}^{avg} . Finally, the average of those reference white pixels is calculated as reference white point $W(R_w, G_w, B_w)$.

The collected white balance data are then transferred to the white balance adjustment unit. The flowchart of white point detection is shown in Fig. 5.

4.3 White Balance Adjustment

First, we collect the data from the white point detection unit and proceed with white balance adjustment. Then, scale factors are calculated according to the reference white point $W(R_w, G_w, B_w)$ for the respective color component as shown in Eq. (6):

$$R_{scale} = Y_w/R_w, G_{scale} = Y_w/G_w, B_{scale} = Y_w/B_w, \quad (6)$$

where, Y_w is calculated using Eq. (7):

$$Y_w = 0.299 * R_w + 0.587 * G_w + 0.114 * B_w. \quad (7)$$

Next, the scale factors are calculated according to GWA as shown in Eq. (8):

$$R_{GWA} = Y_{avg}/R_{avg}, G_{GWA} = Y_{avg}/G_{avg}, B_{GWA} = Y_{avg}/B_{avg}. \quad (8)$$

Finally, decisions are made for selecting proper scale factors based on the color cast over the image. To determine the color cast over the image, we convert the average values of the probably white pixels, Y_{Hist}^{avg} , C_{rHist}^{avg} , C_{bHist}^{avg} from $YCrCb$ to RGB color space as R_{Hist}^{avg} , G_{Hist}^{avg} , B_{Hist}^{avg} . Next, we use Eqs. (9) to (11) to find bluish, greenish, and reddish color casts respectively. Although these equations are based on observation, it is appropriate to use them to find the color cast over the image.

$$B_{Hist}^{avg} + 3 \geq G_{Hist}^{avg} \text{ and } B_{Hist}^{avg} > R_{Hist}^{avg}, \quad (9)$$

$$G_{Hist}^{avg} + 3 > R_{Hist}^{avg} > B_{Hist}^{avg}, \quad (10)$$

$$R_{Hist}^{avg} > G_{Hist}^{avg} > B_{Hist}^{avg}. \quad (11)$$

After finding the color cast, we apply the scale factors. In case of a bluish cast, the scale factors are selected as shown in Eq. (12):

$$R_{factor} = R_{scale}, G_{factor} = G_{scale}, B_{factor} = B_{GWA}. \quad (12)$$

In the case of a reddish cast, the scale factors are selected as shown in Eq. (13):

$$R_{factor} = R_{GWA}, G_{factor} = G_{scale}, B_{factor} = B_{factor}. \quad (13)$$

In the case of a greenish cast, the scale factors are selected as shown in Eq. (14):

$$R_{factor} = R_{scale}, G_{factor} = G_{GWA}, B_{factor} = B_{GWA}. \quad (14)$$

The selected scale factors are applied to the whole image in order to get a white balanced image. The flowchart of white balance adjustment is shown in Fig. 6.

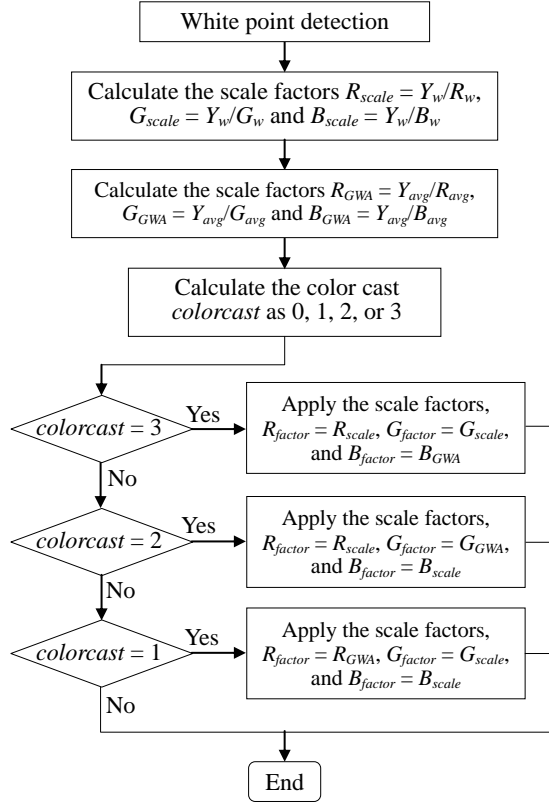


Fig. 6. Flowchart of white balance adjustment.

5. RESULTS

We captured GretagMacbeth ColorChecker images under five light sources and also under household light sources. In addition to checking the stability of the propose method, we captured test images of the same scene with and without ColorChecker. Next we applied the original white balance method based on basic assumptions and the proposed method to the test images. For make more precise comparisons between the methods, we calculated the average chromaticity, $\sqrt{C_r^2 + C_b^2}$, of the achromatic patches of ColorChecker images as objective evaluative values. Besides objective evaluation, we also asked group of people to choose the best image produced by the five methods. The GretagMacbeth ColorChecker image under daylight and the results obtained by applying the five methods are shown in Fig. 7.

To get more precise results, we also captured the images with and without ColorChecker in order to test the stability of our method. The visual results obtained with and without ColorChecker are shown in Fig. 8. Fig. 8 (a1, b1, c1, d1, e1, f1) shows images obtained with ColorChecker and Fig. 8 (a2, b2, c2, d2, e2, f2) shows images obtained without ColorChecker.

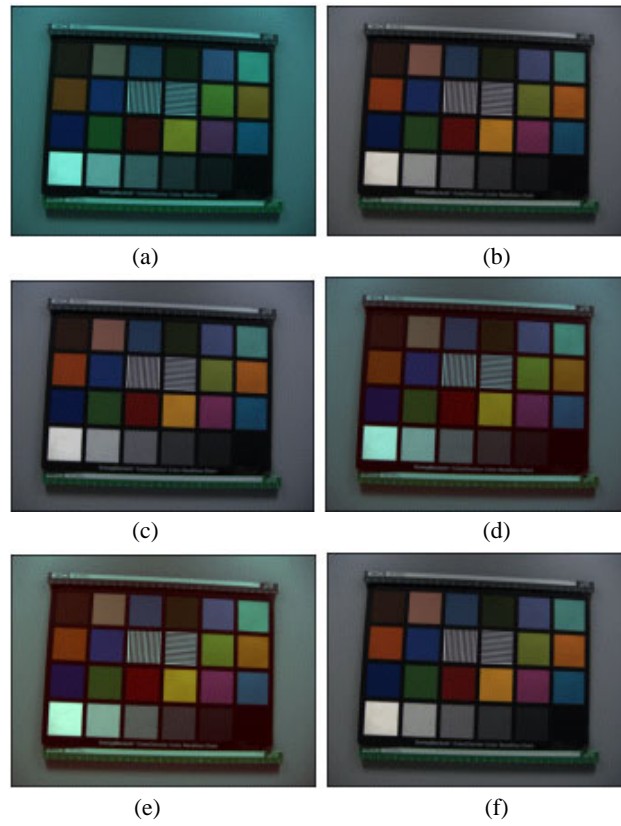


Fig. 7. (a) Original image captured under daylight and results obtained by applying (b) GWM, (c) PRM, (d) FRM, (e) CWBM, and (f) our method.

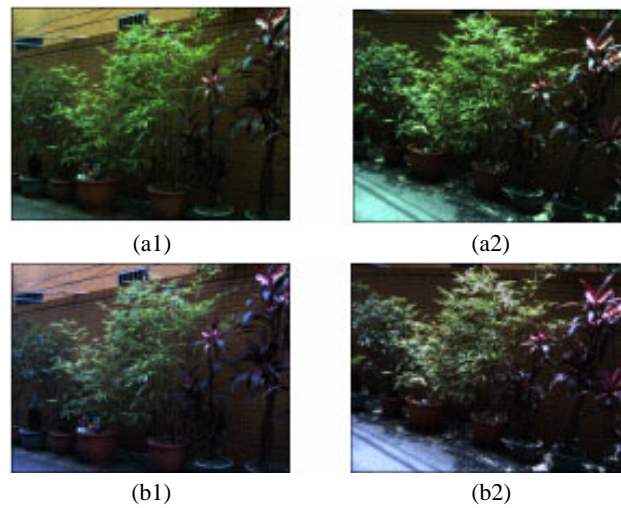


Fig. 8. (a1, a2) Original image, Pots, captured under sunny conditions with (a1) and without (a2) ColorChecker. Visual results obtained after applying (b1, b2) GWM, (c1, c2) PRM, (d1, d2) FRM, (e1, e2) CWBM, and (f1, f2) our method.

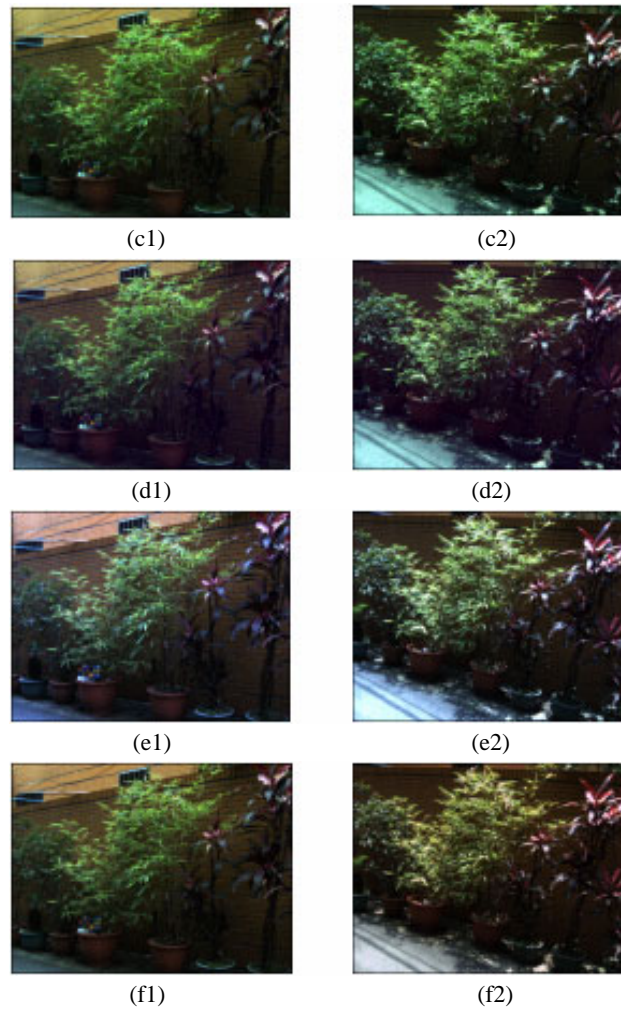


Fig. 8. (Cont'd) (a1, a2) Original image, Pots, captured under sunny conditions with (a1) and without (a2) ColorChecker. Visual results obtained after applying (b1, b2) GWM, (c1, c2) PRM, (d1, d2) FRM, (e1, e2) CWBM, and (f1, f2) our method.

We used the average chromaticity values of the achromatic patches of ColorChecker as objective evaluative values to compare the five methods. The method which forces the chromaticity value closest to zero was assumed to be the best among the five methods. Subjective evaluative values were given by the people in the group.

The objective and subjective evaluative values for all of the test images captured under standard as well as natural and household light sources are shown in Table 2.

The objective and subjective evaluative values for the test images with and without ColorChecker are shown in Table 3. Note that, chromaticity value was calculated just for ColorChecker so in Table 3 (B) row contains the data of the images without ColorChecker, in this case we can just compare the subjective values.

Table 2. Objective and subjective (backed values) evaluative values for all test images.

Image		Original	Simulation				
			GWM	PRM	FRM	CWBM	Our Method
Day Light	(A)	23.47	(4) 1.71	(1) 2.06	(0) 15.62	(1) 4.77	(5) 1.71
	(B)	15.65	(3) 1.26	(0) 15.65	(0) 11.15	(3) 9.97	(3) 1.36
Cool White	(A)	16.57	(2) 1.43	(1) 1.42	(0) 11.50	(6) 3.68	(3) 1.42
	(B)	9.32	(4) 1.71	(0) 7.70	(0) 7.04	(2) 6.26	(3) 3.80
TL84	(A)	16.35	(7) 1.47	(0) 1.42	(0) 11.66	(0) 3.99	(3) 1.29
	(B)	9.61	(5) 1.52	(0) 4.99	(0) 10.99	(0) 3.99	(5) 3.97
INC. 'A'	(A)	20.07	(3) 1.05	(0) 3.44	(0) 14.40	(2) 7.66	(4) 2.08
	(B)	10.56	(4) 1.01	(1) 9.45	(1) 7.60	(2) 5.97	(5) 1.08
HRZ	(A)	33.19	(4) 0.65	(0) 8.66	(0) 22.28	(2) 7.26	(4) 0.76
	(B)	19.91	(3) 1.57	(0) 9.47	(0) 13.36	(3) 9.35	(4) 2.31
Green		20.73	(0) 25.11	(2) 0.73	(0) 20.90	(0) 1.18	(7) 9.11
Steps		20.09	(1) 16.36	(2) 5.79	(1) 19.28	(4) 7.93	(3) 2.97
Cat		15.51	(1) 19.34	(1) 6.30	(1) 16.22	(2) 9.38	(6) 2.64
LCD		10.50	(0) 12.82	(1) 5.00	(0) 11.85	(3) 3.95	(5) 2.50
Fog		24.62	(1) 15.70	(0) 4.62	(0) 16.83	(3) 4.50	(5) 7.93

Table 3. Objective and subjective (backed values) evaluative values for the test images with and without ColorChecker.

Image		Original	Simulation				
			GWM	PRM	FRM	CWBM	Our Method
Doll	(A)	11.21	(3) 7.94	(1) 7.10	(1) 9.49	(6) 9.97	(2) 4.38
	(B)	--	(1) --	(1) --	(0) --	(7) --	(3) --
Foot Ball	(A)	19.16	(1) 12.12	(3) 2.45	(1) 16.56	(3) 9.17	(5) 1.72
	(B)	--	(2) --	(3) --	(1) --	(3) --	(5) --
Lab	(A)	19.23	(7) 2.10	(0) 15.1	(1) 13.25	(1) 8.69	(7) 1.33
	(B)	--	(6) --	(1) --	(1) --	(1) --	(7) --
Pots	(A)	19.02	(1) 26.36	(3) 19.09	(1) 21.00	(3) 23.34	(7) 15.02
	(B)	--	(1) --	(2) --	(1) --	(2) --	(7) --
Building	(A)	23.06	(2) 21.17	(0) 23.06	(1) 23.01	(4) 21.20	(6) 10.21
	(B)	--	(2) --	(0) --	(2) --	(4) --	(6) --

6. CONCLUSION

According to the results of the experiments, we found some serious problems with GWM, PRM, FRM, and CWBA. There were some situations where adjusting the white balance destroyed the consistency of the colors in the image. Therefore, to avoid such

situations, we make use of color cast finding equations. That helps to decide whether apply the white balance. For some subjects, such as greenery, applying any white balance algorithm may result in a bluish cast instead of removal of the original color cast. In our method, we try to get rid of such problems. Under natural light sources and household light sources our method performs the best.

The experimental results show that our method achieved the best performance in both objective and subjective evaluation. The experiments performed with and without Macbeth ColorChecker verify the stability of our method in removing the color cast over the varying object scene. Again the results of varying object and varying light conditions verify the stability of our method can be acceptable for video white balance. The drawback of PRM is overcome by our method by using specific range to find the brightest pixel. Our method works under all possible conditions because the brightest pixel is used to find the range to detect the white pixels under a color cast. In this way, our method either removes the color cast completely or stops white balance adjustment. The complexity of our proposed method is also acceptable.

The unique aspect of our method is the white object purification step and it also opens the new way for the white balance algorithm. Due to the white object purification step, the proposed method successfully finds the white object under any color cast regardless of the light source.

7. FUTURE WORK

We will continue to perform experiments using the white object purification unit. In some rare situations histogram equalization may not be the best way to purify the white object in an image. Another area that needs improvement is the white balance adjustment step. We observed that different colors exhibited different color deviation due to the different light sources and we just adjust rest of the color in the scene by using scale factors calculated from white area of the scene. If we find some way to apply the scale according to the color then we will have a proper way to remove a color cast over the all of the colors in a scene.

REFERENCES

1. R. C. Gonzalez and R. E. Woods, *Digital Image Processing*, Addison Wesley, MA, 1992.
2. M. Fedor, "Approaches to color balancing," PSYCH221/EE362course project, Department of Psychology, Stanford University, U.S.A., 1998.
3. Y. C. Cheng, W. H. Chan, and Y. Q. Chen, "Automatic white balance for digital still camera," *IEEE Transactions on Consumer Electronics*, Vol. 41, 1995, pp. 460-466.
4. J. Chiang and F. Al-Turkait, "Color balancing experiments with the HP-photo smart-C30 digital camera," PSYCH221/EE362 course project, Department of Psychology, Stanford University, U.S.A., 1999.
5. A. V. Durg and O. Rashkovskiy, "Global white point detection and white balance for color images," U.S. Patent #6069972, 2000.

6. T. S. Chiou, "Automatic white balance for digital still camera," Master Thesis, Dept. of Computer Science and Information Engineering, National Taiwan University, Taiwan, 2000.



Varsha Chikane received her M.S. degree in Computer Science and Information Engineering from National Taiwan University, Taipei, Taiwan, in 2004, and her B.C.S. degree in Computer Science from Pune University, Pune, India, in 2002. Her research interests include computer vision, digital processing, and digital still cameras.



Chiou-Shann Fuh (傅樛善) received the B.S. degree from the Department of Information Engineering and Computer Science, National Taiwan University, in 1983, the M.S. degree from Department of Computer Science, Pennsylvania State University, in 1987, and the Ph.D. degree from Department of Computer Science, Harvard University, in 1992. He is a Professor in the Department of Computer Science and Information Engineering, National Taiwan University, Taiwan. His areas of research include computer vision, digital image processing, digital still cameras/digital video camcorders, defect inspection, automatic measurement, and industrial automation.